
This is an electronic reprint of the original article.
This reprint may differ from the original in pagination and typographic detail.

Bai, Long; Xiang, Wenchao; Huan, Siqi; Rojas, Orlando J.

Formulation and Stabilization of Concentrated Edible Oil-in-Water Emulsions Based on Electrostatic Complexes of a Food-Grade Cationic Surfactant (Ethyl Lauroyl Arginate) and Cellulose Nanocrystals

Published in:
Biomacromolecules

DOI:
[10.1021/acs.biomac.8b00233](https://doi.org/10.1021/acs.biomac.8b00233)

Published: 14/05/2018

Document Version
Publisher's PDF, also known as Version of record

Published under the following license:
CC BY

Please cite the original version:
Bai, L., Xiang, W., Huan, S., & Rojas, O. J. (2018). Formulation and Stabilization of Concentrated Edible Oil-in-Water Emulsions Based on Electrostatic Complexes of a Food-Grade Cationic Surfactant (Ethyl Lauroyl Arginate) and Cellulose Nanocrystals. *Biomacromolecules*, 19(5), 1674-1685.
<https://doi.org/10.1021/acs.biomac.8b00233>

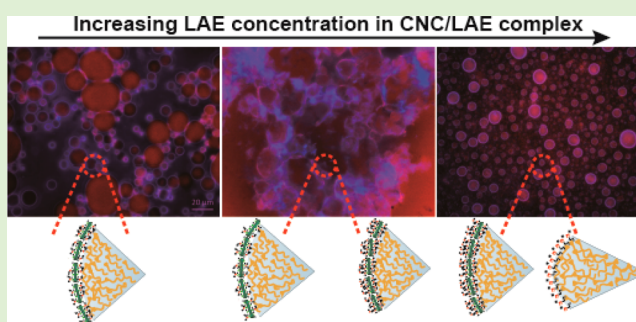
Formulation and Stabilization of Concentrated Edible Oil-in-Water Emulsions Based on Electrostatic Complexes of a Food-Grade Cationic Surfactant (Ethyl Lauroyl Arginate) and Cellulose Nanocrystals

Long Bai,*¹ Wenchao Xiang,¹ Siqi Huan,¹ and Orlando J. Rojas*¹

Bio-Based Colloids and Materials, Department of Bioproducts and Biosystems, School of Chemical Engineering, Aalto University, P.O. Box 16300, FIN-00076 Aalto, Espoo, Finland

Supporting Information

ABSTRACT: We report on high-internal-phase, oil-in-water Pickering emulsions that are stable against coalescence during storage. Viscous, edible oil (sunflower) was emulsified by combining naturally derived cellulose nanocrystals (CNCs) and a food-grade, biobased cationic surfactant obtained from lauric acid and L-arginine (ethyl lauroyl arginate, LAE). The interactions between CNC and LAE were elucidated by isothermal titration calorimetry (ITC) and supplementary techniques. LAE adsorption on CNC surfaces and its effect on nanoparticle electrostatic stabilization, aggregation state, and emulsifying ability was studied and related to the properties of resultant oil-in-water emulsions. Pickering systems with tunable droplet diameter and stability against oil coalescence during long-term storage were controllably achieved depending on LAE loading. The underlying stabilization mechanism was found to depend on the type of complex formed, the LAE structures adsorbed on the cellulose nanoparticles (as unimer or as adsorbed admicelles), the presence of free LAE in the aqueous phase, and the equivalent alkane number of the oil phase (sunflower and dodecane oils were compared). The results extend the potential of CNC in the formulation of high-quality and edible Pickering emulsions. The functional properties imparted by LAE, a highly effective molecule against food pathogens and spoilage organisms, open new opportunities in food, cosmetics, and pharmaceutical applications, where the presence of CNC plays a critical role in achieving synergistic effects with LAE.



INTRODUCTION

Emulsions are integral part of products in food, pharmaceutical, and cosmetic formulations, providing physicochemical, sensory, or biological attributes to products, such as stability, flavor, or texture.¹ Because emulsions are thermodynamically unstable,² their design relies on the identification of strategies to ensure long-term kinetic stability.³ Pickering systems⁴ present a unique way to enable emulsion stability, that is, forming a mechanical barrier with densely packed particles at the oil–water interface,⁵ which may prevent droplet breakage.⁶ Pickering emulsions are generally more stable than emulsions stabilized by traditional surfactants because particles are irreversibly anchored at the oil–water interface upon adsorption,⁷ even at low particle number density.⁸ This is highly desirable for food manufacturers given the need to minimize the concentration of stabilizers in food-grade products. Thus Pickering systems provide a promising alternative in designing and formulating safe and green food emulsions.

Diverse particles have been applied to achieve Pickering emulsions, including graphene oxide,⁹ silica,¹⁰ and modified starch,¹¹ among others. However, most of these particles are

either synthetic or chemically modified, undermining classification as green products. In addition, the growing demand of “label friendly” ingredients to formulate emulsions has increasingly drawn the attention of consumers, further stimulating the study of naturally-derived Pickering stabilizers.¹² Cellulose nanocrystals (CNCs) are cellulosic nanoparticles that are efficient interfacial stabilizers.¹³ Because of their biodegradability, sustainability, and nontoxicity,¹⁴ cellulose nanoparticles are promising in food-grade Pickering emulsions.^{15,16} The adsorption of CNC at the oil–water interface, forming dense interfacial networks, stems from its intermediate wettability and rod-like structure.¹⁷ Capron and coworkers have recently highlighted the utilization of unmodified CNCs to produce CNC-stabilized Pickering emulsions,¹⁸ which can be also tuned according to CNC’s surface charge.¹⁹ Stability is a key indicator of emulsion quality where oil coalescence is unacceptable for consumer products. Commonly, CNC-based Pickering emul-

Received: February 10, 2018

Revised: March 30, 2018

Published: April 2, 2018

sions show creaming or oiling-off after preparation,²⁰ which is due to the large droplet diameter that results from the limited interfacial activity of CNC.²¹ The oil phase usually reported for CNC-based Pickering emulsions usually consists of low-viscosity synthetic oils. In contrast, food-grade oils are generally very viscous; for example, the viscosity of sunflower oil is ~35 times larger than that of dodecane.²² Such high viscosity leads to emulsions of characteristic large droplet size; thus, achieving high stability is quite challenging. To improve the properties of CNC-based Pickering emulsions, the CNC stabilizer has been modified chemically.²³ Surface functionalization of CNC by covalent coupling with various hydrophobic alkyl groups has been successfully performed, leading to stable Pickering emulsions comprising submicron droplets.²⁴ Combining methyl cellulose, tannic acid, and CNC, stable Pickering emulsions can be dried and redispersed in water.²⁵ Overall, chemical treatment or the addition of nonedible components is undesired²⁶ and choosing a facile, eco-friendly approach to formulate highly stable, food-grade CNC-based Pickering emulsions remains a significant hurdle.

Compared with chemical approaches, physical adsorption is a promising alternative to modify CNC. Surfactants can engineer the surface chemistry and colloidal behavior of CNCs, a feasible strategy to tune their emulsifying ability and emulsion stability.²⁷ Cranston and coworkers reported on Pickering systems stabilized by a mixture of CNCs and synthetic cationic surfactants,²⁸ and emulsions with fine droplet sizes were successfully produced.²⁹ Unfortunately, most synthetic cationic surfactants are not edible and may even have a negative impact on the environment, undermining their use in green materials.³⁰

Ethyl lauroyl arginate (LAE), derived from lauric acid, L-arginine, and ethanol, belongs to a kind of amino acid-based cationic surfactant³¹ that has recently been approved as “generally recognized as safe” (GRAS) for certain food applications.³² However, the widespread utilization of LAE in the food industry solely may be limited by its potential to bond to unexpected constituents within the compositionally complicated matrix of food products.³³ LAE can interact strongly with components containing negative charge or hydrophobic groups, leading to adverse consequences for practical application. For example, its interactions may alter the solubility of LAE in aqueous solution, thus affecting the appearance and stability of final products.³⁴ In particular, LAE is known to bind to anionic biopolymers naturally present within the mouth (e.g., mucins), leading to a perceived bitterness or astringency,³³ which is intolerable. Therefore, the use of LAE is likely to largely depend on its interaction with other components within emulsion formulation. On the contrary, LAE also offers the possibility to functionalize other components in emulsions. Herein, we proposed green, physical CNC modification with cationic LAE to electrostatically enhance the negatively charged CNC, endowing better emulsifying ability without altering their sustainable nature. We hypothesize that the colloidal behavior of CNC/LAE complexes can be controllably tuned at the interfaces, thus providing the unique effect on stabilizing fine oil-in-water Pickering emulsions. To our knowledge, this is the first study to use highly viscous, edible oil as raw material to produce concentrated food-grade Pickering emulsions with tunable stability.

A better understanding of the interaction between CNC and cationic LAE will facilitate the rational design and manufacture

of food-grade CNC-based Pickering emulsions. The long-term goal of this research is to introduce improved functionality into high-quality edible and functional Pickering emulsions, for example, with antimicrobial or antioxidant activity.

■ EXPERIMENTAL SECTION

Materials. The food-grade cationic surfactant, ethyl lauroyl arginate (Mirenat-G, LAE, $C_{20}H_{41}N_4O_3Cl$, $M_W = 421.02 \text{ g mol}^{-1}$), containing 10.5% LAE in 89.5% glycerol, was provided by Vedeqsa Group LAMIRSA (Terrassa, Barcelona, Spain). Sunflower oil was purchased from local supermarket without further purification. Nile red and Calcofluor white stain were purchased from Sigma-Aldrich (Helsinki, Finland). Milli-Q water was purified with a Millipore Synergy UV unit (MQ, 18.2 $M\Omega\cdot\text{cm}$) and used throughout the experiments.

Nanocellulose Preparation. CNCs were obtained from ashless cotton fiber filter paper (Whatman 1) by hydrolysis with 64 wt % sulfuric acid at 45 °C and 45 min.³⁵ In brief, the obtained CNC precipitate was rinsed, centrifuged, and dialyzed until the effluent conductivity was $<5 \mu\text{S}\cdot\text{cm}^{-1}$. After filtering, the CNC suspension was stored in the fridge as stock suspension with 1.08 wt % solid content (pH 2.8). The content of sulfate half-ester groups on CNC surface determined by conductometric titration was 0.19 mmol/g, Figure S1. The average dimensions of CNCs were approximately $174 \pm 31 \text{ nm}$ in length and $7 \pm 2 \text{ nm}$ in width, as determined by AFM and ImageJ (Figure S2a).³⁶

CNC/LAE Complex Preparation. Concentrated LAE was diluted to 1.0 wt % by adding MQ water. A range of CNC suspension concentrations were prepared by diluting CNC stock, followed by LAE addition. The final concentration of CNC in the complexes was 0.27 wt %, while that of LAE was varied (0, 0.001, 0.005, 0.01, 0.03, 0.05, 0.1, 0.15, 0.19, 0.2, 0.25, 0.3, 0.4, or 0.6 wt %). In brief, after adding LAE to the CNC suspension, the obtained mixture was mildly shaken (vortex) for 20 s, with further sonication (DT 52/H, Sonorex Digitec, Bandelin, Berlin, Germany) for 5 min at 25 °C. The resulting complexes were stored at ambient temperature prior to analysis. Photographs of the appearance of the complex suspension were taken after 12 h of storage.

CNC/LAE-Stabilized Pickering Emulsions. CNC/LAE-stabilized Pickering emulsions were prepared using equal volume of sunflower oil and the CNC/LAE complex dispersion. The complex dispersions were prepared as above and used immediately after preparation. Practically, sunflower oil was added to the complex dispersion in a plastic tube and sonicated by an ultrasonic device (Sonifier 450, Branson Ultrasonics, Danbury, CT) with a dipping titanium microtip close to the top surface of the emulsions (power level at 40% strength determined by heat balance), alternating 3 s of sonication with 2 s of standby for 60 s.

For visualizing CNCs and sunflower oil simultaneously, the sunflower oil was stained with Nile red before emulsion preparation. 250 μL of Nile red solution (1 mg/mL in ethanol) was added to 5 mL sunflower oil, which was thoroughly mixed at ambient temperature overnight. A similar preparation procedure was used to produce stained emulsions. The dyed emulsion samples were stored at 4 °C before characterization. Photographs of the emulsions were taken within 6 h after preparation. Long-term stability at ambient temperature was monitored, and photographs were taken after 7 and 30 days storage.

Characterization of CNC/LAE Complex. The ζ potential of samples was measured using a Zetasizer Nano (ZS-90, Malvern Instruments, Worcestershire, U.K.). The samples were diluted with MQ water prior to measurement to avoid multiple scattering effects. All measurements were carried out with freshly prepared duplicate samples, and three runs were performed for each sample.

Turbidity. The optical turbidity (at 600 nm) of the dispersions comprising CNC and LAE was measured using a UV-2550 UV-vis spectrophotometer (SHIMADZU, Kyoto, Japan) operated at ambient temperature. The samples were contained within 1 cm path length optical cells. All measurements were carried out on freshly prepared duplicate samples and taken within 2 h of preparation.

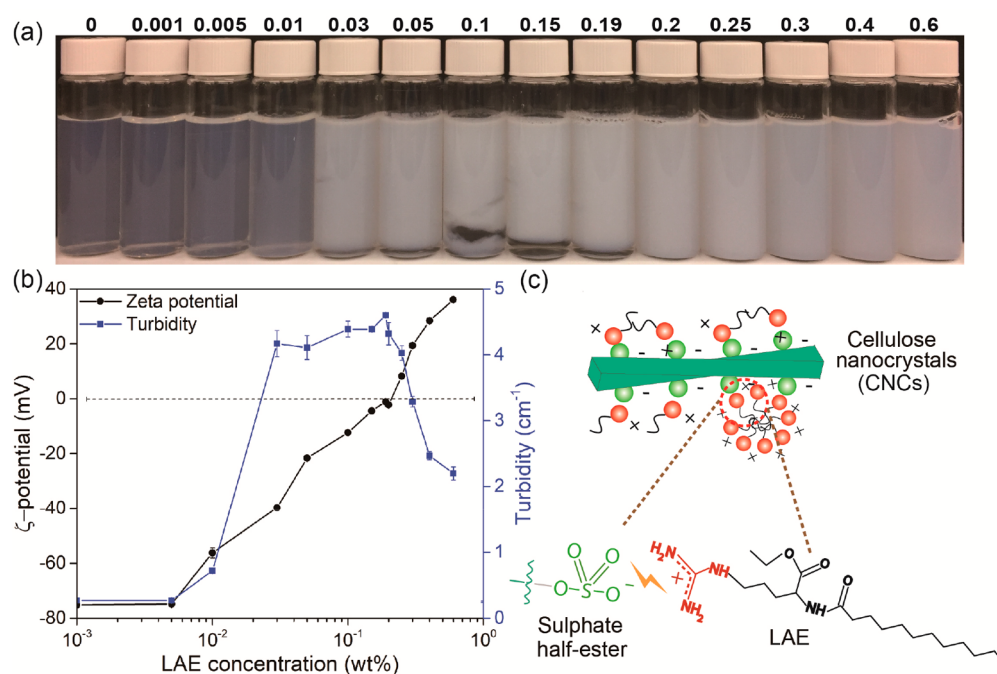


Figure 1. (a) Visual appearance and (b) ζ -potential and turbidity of CNC/LAE complexes in aqueous media at given LAE concentration (wt %). The CNC solids content was kept constant, 0.27 wt %, and the concentration (wt %) of LAE is indicated on top of each sample in panel a. All samples were stored at ambient temperature. (c) Schematic drawing (not to scale) of possible electrostatic binding between the sulfate half-ester on CNC (green) and the guanidinium group of LAE (red).

Isothermal Titration Calorimetry. An isothermal titration calorimeter (VP-ITC, Microcal, Northampton, MA) was used to measure enthalpies of mixing CNC and LAE at 25 °C. Fifty-five 5 μ L aliquots of LAE solution (1.8 wt % LAE and 15.34% propylene glycol, pH 3.2) were injected sequentially into a 1440 μ L titration cell initially loaded with either MQ water or 0.27 wt % CNC dispersion (both containing 15.3% propylene glycol, pH 3.2). The propylene glycol content of LAE and CNC systems was kept the same to avoid heat of dilution effects. Each injection lasted 20 s, with an interval of 240 s between successive injections. The solution in the titration cell was stirred at a speed of 307 rpm throughout experiments. All experiments were carried out on freshly prepared duplicate samples.

Surface and Interfacial Tension. Interfacial tension was measured by the pendant drop method using a contact angle meter (CAM 200, KSV, Finland). Sunflower oil was added to a cuvette, and the transmissivity of the oil container was checked prior to measurement. In brief, a pendant drop of 5 μ L of solution, containing pure LAE or CNC/LAE complex, was formed at the end of a low retention pipet tip (Optifit Tip, Low Retention, Sartorius, Finland) immersed in oil phase. After equilibrating the formed drop for 10 min at ambient temperature, the interfacial tension value was calculated according to the droplet shape recorded during equilibration. The surface tension was measured by the same method using air as the continuous phase. All experiments were carried out on freshly prepared duplicate samples.

Characterization of Pickering Emulsions. Droplet Size. The mean droplet diameter and size distribution of Pickering emulsions were measured using a static light scattering instrument (Mastersizer 2000, Malvern Instruments, Malvern, U.K.). Emulsions were diluted with MQ water prior to analysis to avoid multiple scattering effects. The refractive indices (RIs) of sunflower oil and aqueous phases used in the calculations were 1.47 and 1.33, respectively. The mean droplet diameter of each sample was represented as the volume-weighted mean diameter ($D_{43} = \sum n_i d_i^4 / \sum n_i d_i^3$), which was calculated from the full droplet size distribution. All measurements were performed on freshly prepared triplicate samples and taken within 6 h of emulsion preparation.

Microscopy. The emulsion droplets were visualized by optical microscopy (Leica DM 750, Leica, Germany) with 40 \times and 20 \times objective lens. A drop of emulsion was dripped onto a microscope slide and covered with a glass coverslip (Assistent, Sondheim, Germany). The emulsions were freshly prepared and observed soon after preparation.

The morphology of emulsions after storage (7 days) was examined using confocal laser scanning microscopy (CLSM) with a 60 \times oil immersion objective lens (Leica DMRXE, Leica, Germany). 100 μ L of oil droplets (top layer) was stained with 10 μ L of Nile red solution prior to observation. After homogeneously mixing using a pipet and equilibrating for 10 min at ambient temperature, 6 μ L of dyed samples was placed on a microscope slide and covered with a glass coverslip. The coverslip was quickly fixed by nail polish to avoid evaporation. The excitation and emission spectrum for Nile red were 488 and 539 nm, respectively.

The simultaneous observation of CNCs and sunflower oil in emulsions was imaged by Zeiss Axio Observer optical microscope (Zeiss, Germany) with a 63 \times oil immersion objective. Sunflower oil was stained by Nile red before emulsion preparation. The CNCs were stained by Calcofluor white prior to observation. The procedure used for sample preparation was similar to that used for CLSM. The excitation and emission spectra for Calcofluor white were acquired at 365 and 435 nm, respectively. Merged fluorescence images were processed by ImageJ.

RESULTS AND DISCUSSION

CNC/LAE Complexes. As expected, the colloidal stability, ζ potential, and turbidity of CNC (0.27 wt % dispersion) were affected by the addition of LAE (Figure 1). Initially, the suspensions became increasingly turbid with LAE concentration (0 to 0.01 wt %), but no macroscopic phase separation was apparent (Figure 1a). This is ascribed to the strong electrostatic repulsion, given the high net surface charge of the system at low LAE addition levels (Figure 1b). The ζ potential of the system at 0.01 wt % LAE addition was around -60 mV, lower than that of pure CNC (-81.2 mV) but still significantly

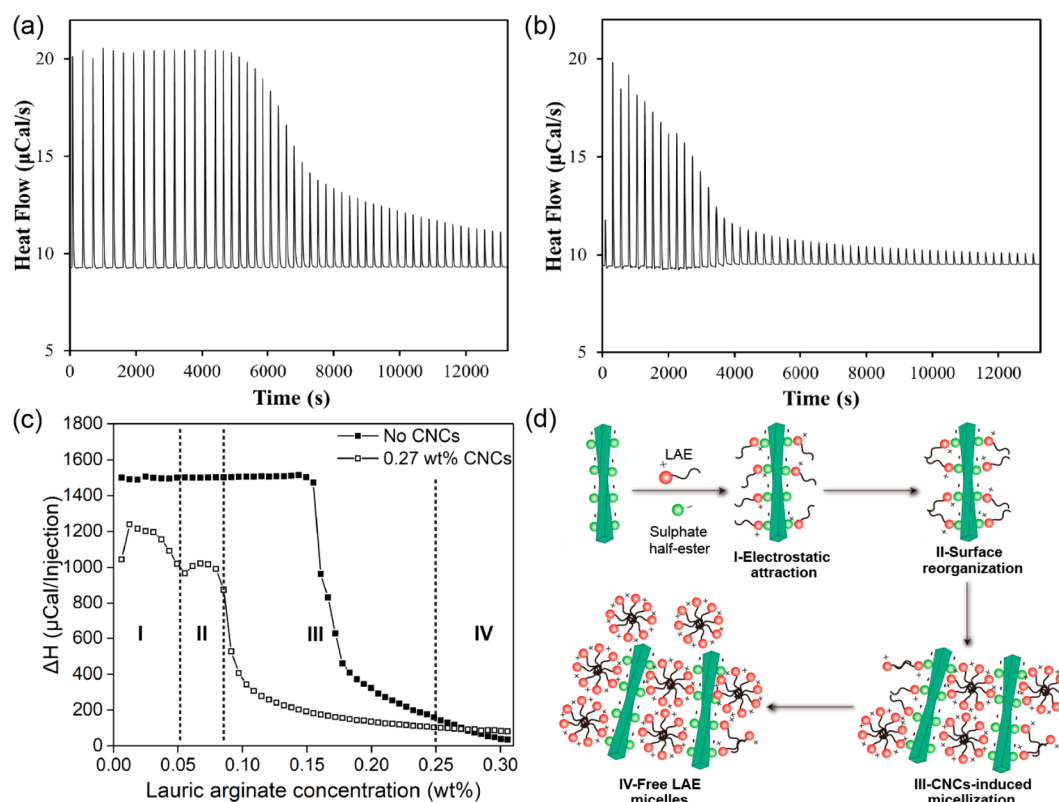


Figure 2. Heat flow profiles from isothermal titration calorimetry (ITC) as a function of time upon injection of LAE solutions to (a) MQ water (no CNC) and (b) 0.27 wt % CNC aqueous suspension. LAE concentrated solution (1.8 wt %) was injected for a total volume of 1440 μL using 5 μL aliquots. The pH of the CNC suspension was 3.2 and temperature was 25 $^{\circ}\text{C}$. (c) Enthalpy change as a function of LAE concentration in water or CNC suspension is shown after integration. Four titration regions were identified in panel c and divided according to LAE concentrations from ITC results (I–IV). (d) Schematic illustration showing (not to scale) the proposed interactions between CNC and LAE corresponding to each region.

high to produce electrostatic stabilization. The turbidity at these low LAE concentrations indicated well-dispersed complexes with little or no aggregation (Figure 1b). At intermediate LAE concentrations (0.03 to 0.20 wt %), large aggregates formed and phase separation was observed (Figure 1a), as explained by CNC charge neutralization and possible bridging of the anionic CNC nanorods and the cationic LAE micelles. The turbidity at these LAE concentrations sharply increased, reaching a maximum at 0.19 wt %, which indicated the formation of aggregates that scattered light strongly. Further increase in LAE concentration (≥ 0.25 wt %) enabled redispersion, as judged by the absence of phase separation; the suspensions were homogeneous and displayed relatively low turbidity. In this concentration regime the complexes were large and displayed strong light scattering but did not settle under gravity. As for the variation in turbidity, the transition point after which the turbidity decreased is related to LAE micellization in the CNC/LAE suspension. Originating from the increased net charge, the formed micelles provide electrostatic repulsion between the complexes. The onset of concentration at which turbidity started to decrease took place at approximately 0.20 wt % LAE, where free LAE micelles form in the aqueous suspension. This value agrees with ITC results (Figure 2) that indicated a very close figure, 0.19 wt % LAE concentration. On the contrary, charge reversal occurred for the associative structures at high LAE concentrations, owing to the formation of LAE admicelles or micelle-bound structures that formed on CNC (Figure 1c). Accordingly, the decreased number of available free sulfate half-ester groups on the CNC,

which otherwise may form electrostatic bridges, as has been observed for other systems, promoted the redispersion of the associated structures.³⁷

Notably, the isoelectric point occurred around 0.19 wt % LAE, which was much higher than the value predicted on the basis of charge neutralization (equal molar number for sulfate half-esters on CNC and LAE charges, at 0.022 wt %). This is explained by the balance between free and bound LAE, which governs the amount of LAE that is actually adsorbed on CNC and effective in charge neutralization. Moreover, it is expected that the presence of electrolytes can further increase the required surfactant excess for charge neutralization.³⁸

AFM imaging was used as indirect evidence to elucidate the changes in the microstructure of pristine CNC and their complexes at various LAE concentrations (Figure S2). While the effect of water removal (drying) in acquiring the AFM images is important, one can speculate on some generic observations that point to distinctive changes in the CNC/LAE complexes. At low LAE loadings (0.01 and 0.05 wt %, Figure S2b,c), the system evolved from well-dispersed, individual CNCs to aggregates that coexisted with laterally assembled CNC nanorods. This is attributed to the decreased electrostatic repulsion between the complexes as the LAE molecules interacted with the nanorods (Figure 2d). However, the LAE concentration in this stage was not sufficient to fully cover the CNCs or induce interparticle bridging. Therefore, individual nanorods were still observable (AFM imaging). At intermediate LAE concentrations (0.1 and 0.19 wt %, Figure S2d,e), large, irregular and sheet-like clusters were formed owing to the fact

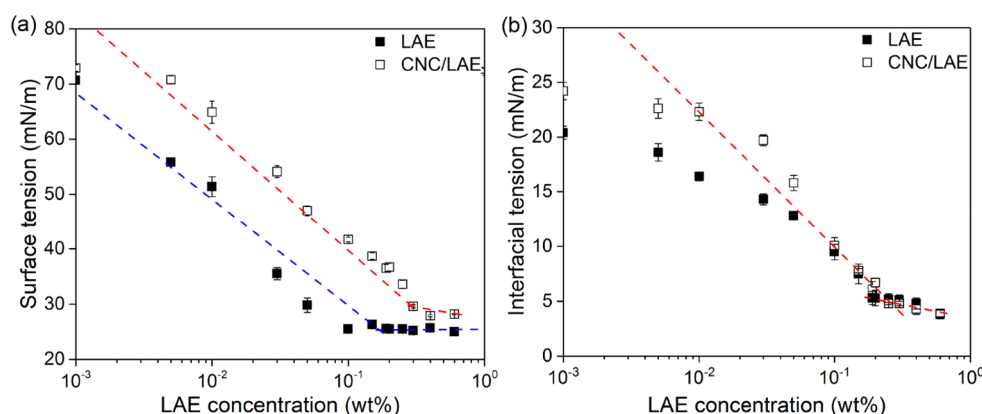


Figure 3. (a) Surface (air–water) and (b) interfacial (sunflower oil–water) tension of pure LAE and CNC/LAE systems at different LAE concentrations. The CNC concentration was 0.27 wt %. In (a) and (b), the upper, red dotted lines intersected at the apparent value for CNC/LAE association concentration. In (a), the lower blue dotted lines intersected at the expected CMC value for LAE. All measurements were performed at ambient temperature.

that electrostatic repulsion between the complexes was extremely low at these concentrations. In addition, the bridging and intermolecular assembly of CNC via hydrophobic interactions between alkyl groups of LAE bound on the CNC surface could promote complex aggregation (Figure 2d). At further increased LAE concentration (Figure S2f), complex aggregation was still observed but displayed a characteristic reduced size. This is likely the result of free LAE micelles that existed in the aqueous phase and that were effective in separating the aggregates, as discussed above and schematically shown in Figure 2d, IV. The proposed morphological transitions can also be partially explained by the energetically favorable formation of complex structures in solution.³⁹ Overall, taken the AFM images as indirect evidence, there is an indication of the redispersion of CNC/LAE complexes at high LAE concentrations. This is in agreement with the turbidity measurements which demonstrate the possibility of tunable colloidal properties.

Isothermal titration calorimetry (ITC) was applied to reveal the different interaction regimes based on the evolution of enthalpy changes, ΔH , upon titration of an aqueous CNC suspension with LAE (Figure 2). As a reference, the typical heat flow versus time profile after the stepwise addition of concentrated LAE solution into water is shown in Figure 2a, similar to other reported results⁴⁰ but noting variations originating from the measuring conditions and instrument used.⁴¹ The relationship between enthalpy changes, measured by the titration with LAE of either water or CNC aqueous dispersions, was derived from the calculation (integration) of the heat flow versus time profiles (Figure 2c). According to Figure 2c, the critical micelle concentration (CMC) of LAE determined from the inflection point in the ΔH versus concentration profile was 0.18 ± 0.01 wt %.⁴⁰ In the presence of 0.27 wt % CNC (Figure 2b), a distinct change in the ΔH –time profile occurred, indicating strong interaction between CNC and LAE. From the CNC/LAE profile shown in Figure 2c, four interaction regimes can be distinguished, which are shown schematically in Figure 2d.

Region I at LAE < 0.05 wt %. In this region, in the presence of CNC, the enthalpy change was endothermic, but it was considerably less compared with the values obtained from similar experiments in the absence of CNC (pure water). This implies a net exothermic interaction between LAE and CNC given the strong electrostatic attraction between negative

sulfate half-ester groups on the surface of the cellulose nanorods and the positive guanidinium headgroups of LAE.⁴² It can be speculated that the electrostatically driven binding leads to the formation of adsorbed LAE on the surface of CNC (Figure 2d), probably in a non-associated form, given that the concentration was too low for LAE to otherwise associate as micelles or admicelles.

Region II at 0.05–0.08 wt % LAE. In this regime, the enthalpy change was endothermic in the presence of CNC but less than that observed at the lower LAE concentrations. This indicates still exothermic (electrostatic) interactions between LAE and CNC. As the ΔH showed a plateau in this region, the reorganization of LAE molecules on CNC surface was also considered to be induced by hydrophobic interactions of alkyl chains so as to reduce the thermodynamically unfavorable contact of LAE tails with water molecules,⁴³ as shown in Figure 2d. At the end of this regime, CNC should be fully covered with LAE molecules. A four-fold higher value was determined for LAE saturation concentration on CNC surfaces from ITC experiments compared with the theoretical value (0.022 wt %), which indicates that not all LAE molecules absorbed after injection but partitioned at the air–water interface, thereby increasing the amount of LAE needed for CNC charge neutralization.⁴⁴ A dynamic partitioning equilibrium may exist for LAE molecules between the CNC surfaces, air–water interface, as well as free and associative structures in solution.

Region III at 0.08–0.25 wt % LAE. The enthalpy change was gradually decreased at further LAE addition levels, possibly indicating little direct interaction between CNC and the surfactant molecules. In this regime it is possible that bilayer, patchy bilayer,⁴⁵ or admicelle morphologies occurred, driven by the strong interactions of alkyl chains of LAE, via positive-cooperative binding,⁴⁶ as illustrated in Figure 2d. The increased local concentration of LAE molecules around the cellulose nanorods also promoted the formation of LAE micelles on CNC surface. This is akin to a polymer-induced micellization due to locally increased surfactant concentration around the CNC surface and occurred at a concentration lower than the CMC of the surfactant.⁴⁷ The aggregation and bridging of micelles bound to CNC may have also occurred in the form of large aggregates, containing several cellulose nanoparticles. Because CNC is a rigid, rod-like nanocrystal, it is unlikely to wrap around LAE micelles, as flexible polymers do.⁴⁸ Thus it is

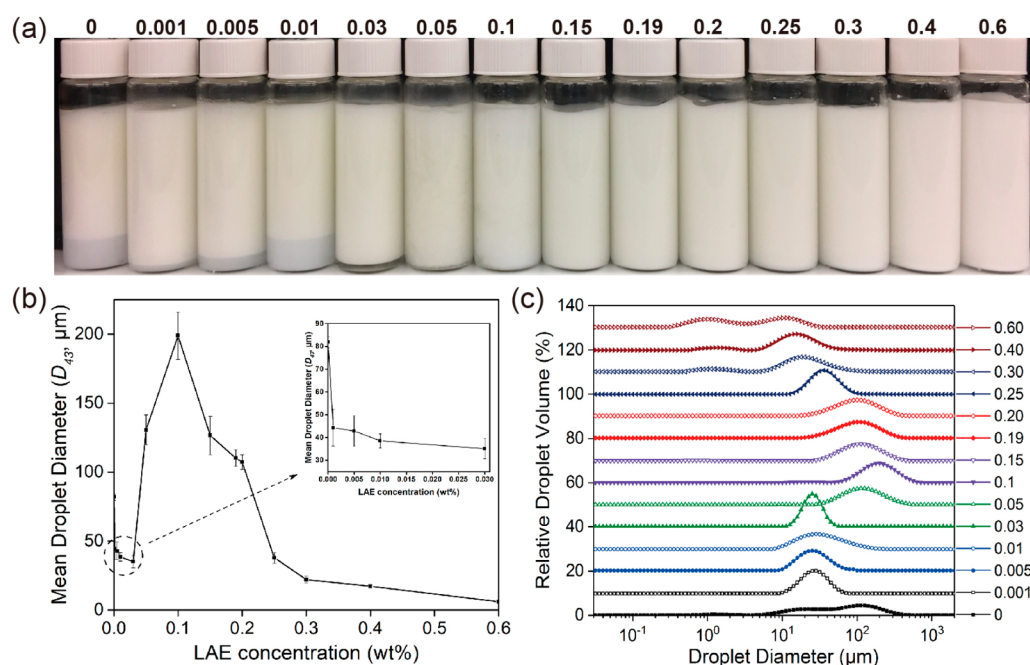


Figure 4. (a) Visual appearance, (b) mean droplet diameter (D_{43}), and (c) droplet size distributions of CNC/LAE-stabilized oil-in-water Pickering emulsions containing 50% v/v sunflower oil at different LAE loadings. The concentration (wt %) of LAE is indicated on top of each sample in panel a. The photographs in panel a were taken within 3 h of emulsion preparation. The insert in panel b is an enlargement of the indicated area at low LAE concentration. To facilitate comparison in panel c, the profiles for the different systems (as indicated by the LAE concentration on the right) were shifted in the vertical axis.

suggested that CNC rods were bridged by LAE micelles, given that this is energetically favorable.

Region IV at LAE > 0.25 wt %. In this regime and with increasing LAE concentration, the enthalpy change became progressively less endothermic, following a similar trend as that observed in experiments with water but at higher LAE concentrations, suggesting that the enthalpy value was only related to the dilution of LAE micelles. It can therefore be reasonably postulated that the concentration of free LAE molecules in aqueous phase increased above the CMC in this region so that any additional LAE titrated into the reaction cell remained in the form of free micelles.

Finally, we note the limitations of the ITC technique because it only presents the overall enthalpy change within the system, meaning that it is incapable of accurately isolating the contributions of micelle dissociation, monomer binding, micelle binding, as well as aggregation and bridging of CNCs.⁴⁸ Therefore, other complementary analytical techniques may be relevant to further inquire into the interactions between CNC and LAE.

Surface and Interfacial Behavior of CNC/LAE Systems.

The surface (air–water) and interfacial (sunflower oil–water) behavior of the complexes was investigated by experiments with the pendant drop technique (Figure 3). As shown in Figure 3a, the surface tension of pure LAE decreased gradually with concentration until reaching the CMC; it then leveled off to a plateau value of ~ 26 mN/m. The CMC of LAE was determined to be 0.19 wt % from the intersection between the extrapolated profiles from high and intermediate LAE concentrations, very close to the CMC determined from ITC. In the presence of 0.27 wt % CNC, an increase in surface tension at similar LAE loadings resulted in the entire curve shifting to the right, which showed a plateau at 28 mN/m. The apparent CMC value of the complex increased to ~ 0.3 wt %

(intersection of red dotted lines, Figure 3a). This behavior is different from flexible or long-chain fibers that can shift the CMC to lower concentration by promoting surfactant partitioning at the air–water interface.⁴⁹ In contrast, short rod-like CNC can bind LAE molecules by electrostatic interactions that may not be able to wrap around the nanoparticles, thereby reducing the number of LAE molecules that are partitioned at the air–water interface; namely, the amount of total LAE needed to form free micelles in water is increased.

The interfacial tension measured for the complexes with LAE at low concentration (<0.05 wt %) was larger than that in the absence of CNC (Figure 3b). However, the two profiles cross at higher concentrations, indicating that the complexes could significantly reduce the interfacial tension at sunflower oil–water interface. This is a key factor affecting emulsion formation. Notably, CNC alone can actually reduce the interfacial tension at the oil–water interface, but higher concentrations are needed.²⁸ It can therefore be inferred that the low amount of CNC (0.27 wt %) used in the current system hardly affected the interfacial tension, leading to the fact that the enhanced surface activity resulted from hydrophobic modification of CNC with LAE. It was also the main reason facilitating the partition of the complexes at the oil–water interface. Overall, the investigation of the properties of CNC/LAE complexes in suspension and at the oil–water interface indicated their possibility to act as an interfacial stabilizer in Pickering systems.

CNC/LAE-Stabilized Pickering Emulsions. Pickering emulsions prepared from equal volume of CNC/LAE suspensions and sunflower oil (water-to-oil ratio, WOR = 1) were prepared using 0.27 wt % CNC and various LAE concentrations (Figure 4). As shown in Figure 4a, Pickering emulsions stabilized with CNC were possible but unstable. The

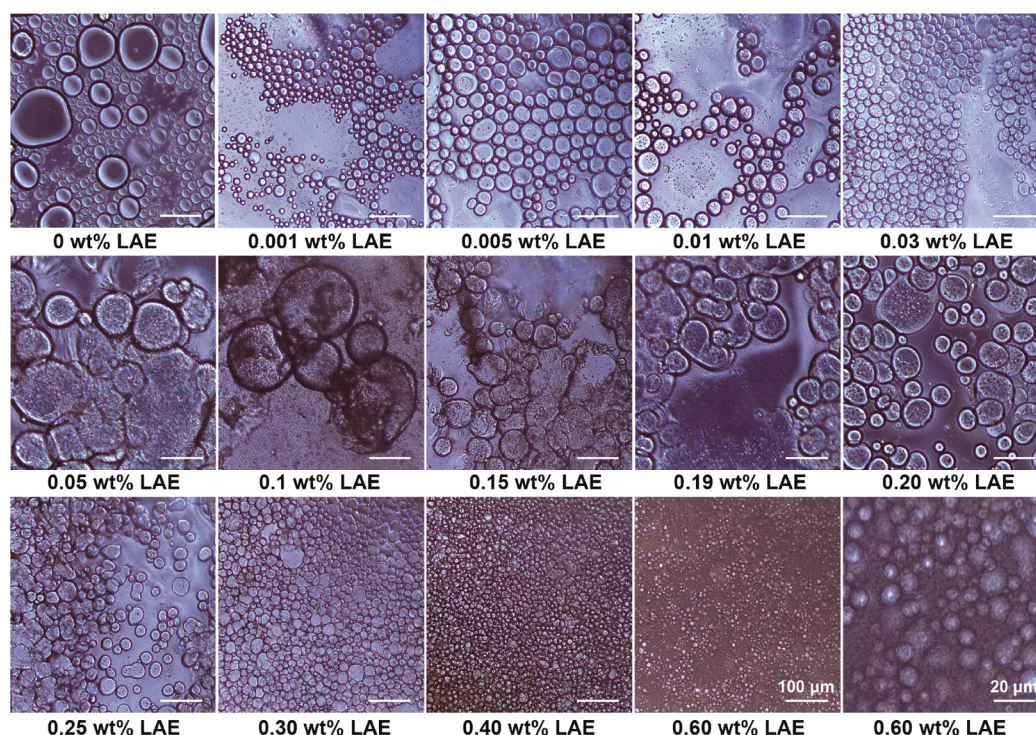


Figure 5. Optical micrographs of CNC/LAE-stabilized Pickering emulsions containing 50% v/v sunflower oil at different LAE loadings. LAE concentration is indicated below each image. The scale bar is 100 μm . A micrograph of the emulsion stabilized with CNC/LAE (0.6 wt % LAE) is shown with higher magnification (scale bar of 20 μm). All samples were stored at ambient temperature before testing.

coalesced oil adhered to the vial surface soon after preparation. At such low CNC concentration and relatively high oil volume, the oil droplets were difficult to be observed.¹⁸ In the presence of LAE, the complexes with CNC led to stable (no oil coalescence) oil-in-water Pickering emulsions. Slight creaming with the formation of a bottom-aqueous serum was displayed only at low LAE concentrations (0.001 to 0.03 wt %), indicating the good emulsifying ability of CNC/LAE complexes for stabilizing the sunflower oil, which is rather viscous.

Figure 4b indicates that the mean droplet diameter (D_{43}) of the Pickering emulsions could be tuned by the amount of LAE in the complexes. At intermediate LAE loadings, the net surface charge of the complexes was negligible (Figure 1b); therefore, the absence of a strong electrostatic repulsion prevented the stabilization of the newly formed Pickering droplets; that is, coalescence occurred during droplet formation. Additionally, it is possible that the large size of the complexes limited the diffusion from the aqueous phase to the newly formed interfaces, leading to significant coalescence of the oil droplets formed soon after sonication. Nevertheless, the emulsions appeared to be homogeneous at such concentrations even if they displayed large oil droplet sizes, owing to the high viscosity of the oil and prepared emulsions, which could temporarily restrict the ascending movement of droplets during short storage time (see Figure S3 for the apparent and shear viscosity of CNC/LAE-stabilized Pickering emulsions under shear condition typical of food processing). It can be expected that a suitable coverage at the interface will reduce coalescence once sufficient CNC/LAE is adsorbed at the interface. For instance, at low LAE concentrations, the surface charge of the complexes was sufficient to prevent droplet coalescence, and the higher diffusion rate of the small complexes could also contribute to oil droplet stabilization during emulsification, thereby producing smaller droplets compared with those observed for

emulsions at intermediate LAE concentrations. However, it should be noted that the droplet size was still large, possibly due to the strong surface charge of the complexes that prevented better packing at the interface covering the oil droplet. Increasing the LAE concentration to >0.25 wt %, small complexes formed, the electrostatic repulsion and the free LAE molecules in water could all work synergistically to stabilize Pickering emulsions with very fine droplet sizes without creaming. The droplet size at high LAE concentration was smaller than that determined at low LAE loading (Figure 4b), which may be due to the reduced interfacial tension at the oil–water interface and the net surface charge. That is, the complexes formed at high LAE loadings were more efficient to reduce the interfacial tension at the oil–water interface (Figure 3b), thereby producing smaller droplets under similar emulsification conditions. Moreover, the relative lower surface charge at high LAE levels resulted in more packed arrangement of the complexes at the interface (Figure 1b), effectively restricting droplet coalescence.

Figure 4c shows the droplet size distribution of Pickering emulsions formulated with CNC and different amounts of LAE. The droplet size distribution produced for LAE concentrations between 0.001 and 0.25 wt % was unimodal. However, between 0.05 and 0.2 wt %, the width of the peaks was larger compared with that at other concentrations, indicating the effects of size polydispersity. This significant variation of droplet diameter may result from the uncontrolled coalescence of newly formed droplets during formation, which could be further evidenced by droplet morphology (Figure 5). At high LAE loadings, the droplets showed a bimodal distribution, implying possible differences in the mechanism of droplet formation, as will be discussed in detail in the following section.

Emulsion Morphology. Figure 5 shows the morphology of CNC/LAE-stabilized Pickering emulsions. All images were

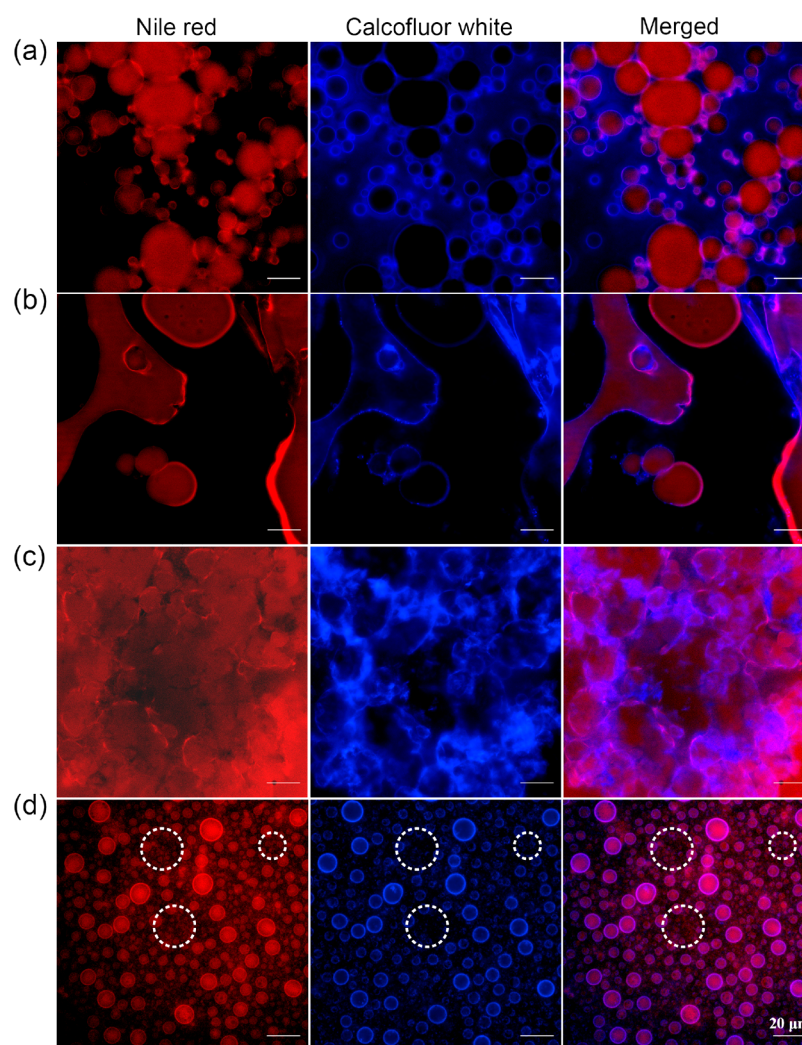


Figure 6. Fluorescence micrographs of CNC/LAE-stabilized Pickering emulsions containing 50% v/v sunflower oil in the presence of CNC (0.27% concentration) and LAE at (a) 0.001, (b) 0.05, (c) 0.1, and (d) 0.6 wt %. The left and middle rows are the images obtained from staining the oil phase and from the dyed CNCs, respectively. The right row is a composed image after merging the other two. The sunflower oil was stained with Nile red before emulsion preparation, and CNCs were dyed with Calcofluor white prior to observation. The dotted circles in panel c are used to highlight the oil droplets. The scale bars correspond to 20 μm . All samples were stored at ambient temperature.

taken within 3 h after preparation to avoid macroscopic instability. The droplets were spherical in shape and their size presented similar evolution (Figure 4b). Not surprisingly, for several samples, the size of the droplets assessed by optical micrographs was slightly different from that determined by light scattering. Figure 5 also shows that the emulsion containing only CNC was nonhomogeneous, indicating the poor stabilization of the highly charged CNC. When mixed with LAE at concentrations <0.03 wt %, the droplets were well-dispersed and showed similar droplet diameters, which are in agreement with observations in Figure 4b. This confirms that LAE can promote the formation of CNC-based Pickering emulsions, even with little addition. After adding LAE over 0.05 wt %, the size of the droplets increased sharply: large oil droplet clusters were formed in the emulsions showing polydisperse distributions. Thick droplet boundaries could be distinguished (0.19 wt % LAE), implying that interfacial layers formed by the complexes were sufficient to resist droplet breakage during preparation and short storage time. After further increasing LAE concentration beyond 0.25 wt %, the trend in oil droplet diameter reversed and it became smaller and homogeneous,

demonstrating the high efficiency of the complexes in producing Pickering emulsions. Droplets with sizes on the order of 2 μm could be observed (see profiles in Figure 4c and the inset of Figure 4b), confirming the formation of a bimodal system. Overall, the incorporation of LAE into a CNC suspension, forming CNC/LAE complexes, greatly improved the emulsifying ability of cellulose nanoparticles and led to stable Pickering emulsions with tunable droplet size.

Emulsion Stabilization Mechanism. The approximate O/W interfacial area and CNC surface area were determined to inquire into the possible emulsion stabilization mechanism. According to previous work,¹⁸ the total % coverage C of CNC-stabilized droplets can be determined as follows

$$C = \frac{m_p D}{6h\rho V_{\text{oil}}}$$

where m_p is the mass of CNC/LAE complex, D is mean droplet diameter (D_{43}), h is the thickness of the CNC/LAE adsorbed complex (6 nm obtained from AFM), ρ is the density of the complex (1.6 g/cm³), and V_{oil} is the volume of oil used in the emulsion (sunflower oil). It should be noted that the density ρ

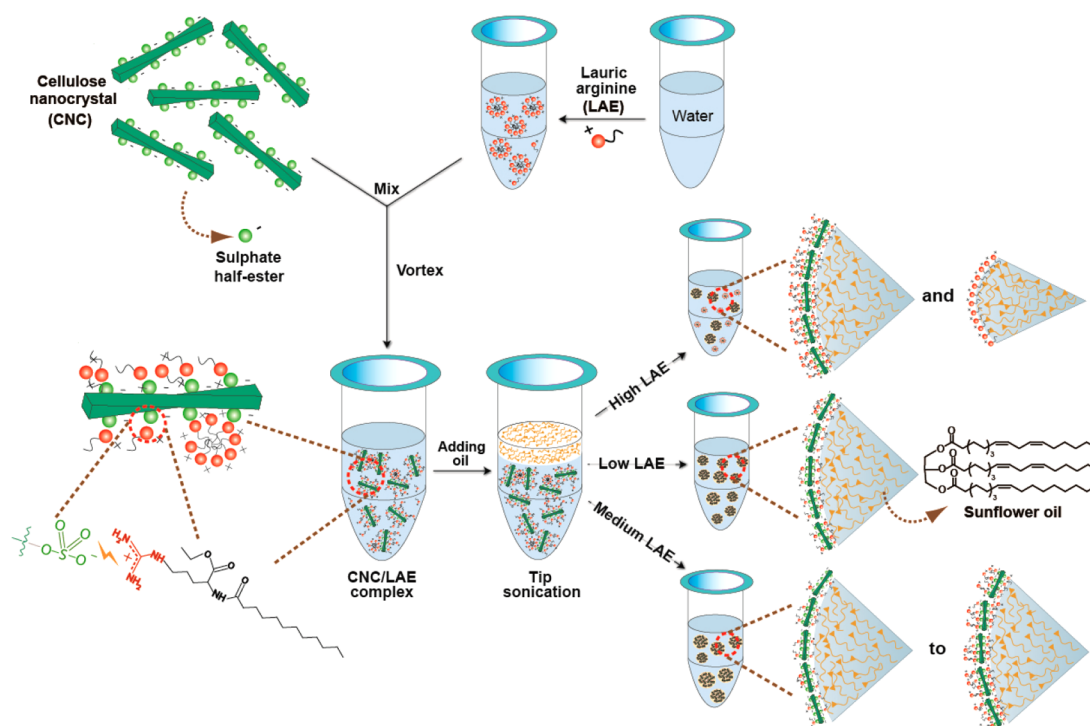


Figure 7. Schematic illustration (not to scale) of the formulation, preparation, and oil droplet stabilization via electrostatic interactions involving CNC and LAE. The proposed Pickering emulsion stabilization mechanism at different LAE loading levels is introduced.

used in this calculation for the associative structures was taken as that of pure CNC, which is only an approximation (the actual density is expected to decrease with LAE addition). The volume of water and oil phases in the emulsions is equal (water-to-oil ratio, WOR = 1). As such, if the oil droplet surface was fully covered by the complexes, then the minimum mean diameter should be $\sim 21 \mu\text{m}$. On the contrary, $\sim 84\%$ surface coverage has been considered as sufficient to produce stable Pickering emulsions with cotton-derived CNC.⁵⁰ On the basis of this assumption, the amount of complexes used in this work was sufficient to stabilize droplets as small as $\sim 25 \mu\text{m}$.

We followed the location of CNC to explore the stabilization mechanism in the Pickering emulsions. CNC was dyed with Calcofluor white, rendering it blue in the microscope images, and oil was stained with Nile red (shown in red). Figure 6 shows the micrographs of stained oil droplets, dyed CNC, and corresponding merged fluorescence images. The possible stabilization mechanism for Pickering emulsion stabilized by the complexes is shown schematically in Figure 7. At low LAE addition (Figure 6a), CNCs were both adsorbed at the oil–water interface and distributed in the aqueous phase. The distribution of CNC in the aqueous phase may be ascribed to the strong electrostatic repulsion between CNCs, resulted from the high residual negative charge after interacting with LAE molecules. Such factors limited CNC adsorption at the interface. Furthermore, our calculation above suggested that less CNC is needed for full coverage of the droplets. Considering the ζ -potential of the emulsions (Figure S4), we suggest that the droplets were stabilized by the complexes containing partially neutralized CNC at low LAE addition (Figure 7). This assumption may be further confirmed from the ITC experiments and by the fact that the emulsions were unstable when CNC was used alone.¹⁸ Adding intermediate amounts of LAE (Figure 6b,c), CNC adsorbed at the oil–water

interface; however, in this case the droplets clustered, forming large oil domains. It is worth noting that no CNC was found dispersed in the aqueous phase. Although the complexes were all adsorbed at the oil–water interface, their aggregated forms resulted from low surface charge and decreased effective coverage, leading to much larger droplet sizes than predicted. As shown in Figure S4, emulsions prepared with 0.05 wt % LAE showed droplets that were negatively charged, but charge reversal occurred at 0.1 wt %, which may be correlated to the ITC results (Figure 2); that is, CNCs were nearly neutralized at 0.05 wt % LAE, but bilayer or admicelles formed on the surface of the CNC at 0.1 wt % LAE. Accordingly, we speculate that at increased LAE concentrations the complexes that stabilize the droplets may undergo a transition from nearly neutralized CNC aggregates to CNC aggregates containing adsorbed surfactant bilayers or admicelles (Figure 7).

The fluorescence micrograph in Figure 6d indicates a bimodal system, also shown in the optical micrographs. As can be seen in this figure, most of the large droplets and part of the small ones displayed clear blue contour, implying that CNC was adsorbed at the interface. Notably, no blue contours around some of the small droplets were observed, possibly indicating that these droplets were not stabilized by the complex but by the surfactant alone. Indeed, the calculated minimum droplet diameter (even at 100% coverage) indicated that CNC alone may not be able to stabilize all such small droplets. To investigate the composition of the interfacial layers in small droplets, sunflower oil-in-water emulsions were prepared in the absence of CNC, with LAE alone (Figure S5). As shown in Figure S5, the prepared emulsions, with or without CNC, showed similar droplet diameter, $\sim 1 \mu\text{m}$. We note that free LAE molecules were present in the aqueous phase at LAE concentration $< 0.25 \text{ wt } \%$ (Figure 2d). Consequently, it is reasonable to propose that the oil droplets

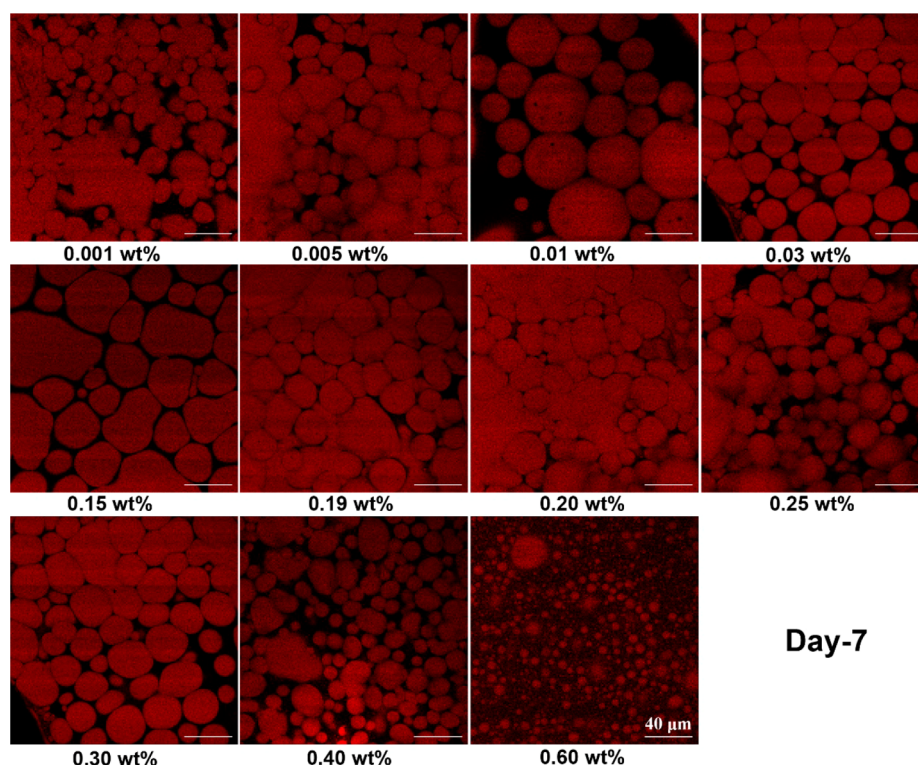


Figure 8. CLSM images after storage for 7 days of CNC/LAE-stabilized Pickering emulsions containing 50% v/v sunflower oil at fixed CNC concentration (0.27%) and given LAE loading, as indicated below each image. The oil phase was stained with Nile red prior to observation. The scale bar corresponds to 40 μm . All samples were stored under ambient conditions.

were stabilized by both the complexes containing fully covering CNCs, and by LAE surfactants, producing a biomodal emulsion system (Figure 7). Such dual-droplet system has not yet been fully explored but may be of potential interests in the design and manufacture of heterogeneous emulsion-based materials.

The observations in the present system differ from results obtained with synthetic cationic surfactants in the presence of CNC, which at high surfactant loadings preferentially stabilized the oil–water interface (stronger affinity to the interface).³⁸ However, a consideration to be highlighted is the type of oil used: In the noted work, dodecane was the oil phase (equivalent alkane carbon number, EACN = 10), which favors better surfactant adsorption than sunflower oil (EACN \approx 14). Indeed, tests with dodecane oil indicated agreement with the previous observations (Figure S6): In the merged micrographs, the CNC/LAE complexes were distributed non-homogeneously in the aqueous phase rather than adsorbed at the oil–water interface. Thus, the fine dodecane droplets were stabilized by LAE alone. Considering the dramatic difference between dodecane and sunflower oil and the above results, we hypothesized that sunflower oil affected the behavior of the Pickering emulsions, inducing a synergistic stabilization via the CNC/LAE complexes as well as LAE molecules at high enough LAE concentrations.

Long-Term Stability. The long-term stability of sunflower oil-in-water Pickering emulsions stabilized by the CNC/LAE complexes was evaluated after storage for 7 and 30 days (Figure S7). Emulsions stabilized by CNC only showed extensive oil coalescence after storage, indicating poor stability. In the presence of 0.05 and 0.1 wt % LAE, significant oil coalescence was observed, with large oil droplets dispersed within and on the top of emulsions after 7 days. This is ascribed to the limited

electrostatic repulsion that otherwise prevents droplet coalescence (Figure S4). After 30 days, the oiling-off of these emulsions was obvious (Figure S7). For other emulsions (except for 0.6 wt % LAE), only creaming was observed after storage. In particular, there was no creaming for emulsions stabilized by the CNC/LAE complex containing 0.6 wt % LAE, even after 30 days. Thus this system was best in emulsifying and stabilizing the Pickering emulsion. It is well known that droplet creaming to oil coalescence is more sensitive in large-droplet systems.⁵¹ However, although the diameter of droplets in the current Pickering emulsions was quite large, at least when compared with other Pickering systems, the emulsions were nevertheless extremely stable to coalescence at the given LAE concentration: The complexes resisted interfacial disruption by gravity, collision, and other effects during storage. On the contrary, the strong electrostatic repulsion between droplets resulted from a high surface charge that contributed to the resistance to oil coalescence. It is worth noting that the emulsion with 0.6 wt % LAE (in the absence of CNC) was stable for 7 days but showed oil coalescence after 30 days (Figure S8). Thus, the combination of CNC and LAE leads to stable emulsions, much more effectively than when CNC or LAE are used alone.

Figure 8 shows the CLSM images of Pickering emulsions after 7 days of storage. For samples containing 0, 0.05, and 0.1 wt % LAE, significant oil coalescence occurred. From Figure 8, oil droplets kept their shape and were distributed homogeneously during storage in most of emulsions, except those containing 0.15, 0.19, and 0.20 wt % LAE, which also formed irregular droplets at the high oil loading. The diameter of the droplets was similar to that obtained by light scattering and indicated clustering, given the high oil concentration and large

droplet diameter. The droplets observed in CLSM confirmed the stability of Pickering emulsion after storage. In summary, no phase separation was visible for CNC/LAE-stabilized Pickering emulsions after long-term storage, making them suitable for food-grade emulsion formulations. Remarkably, oil-in-water Pickering emulsions containing concentrated edible oil that is stable against oil coalescence during storage has not been reported, to our knowledge; therefore, the results in this study open an opportunity for CNC for the formulation of such systems.

CONCLUSIONS

Stable sunflower oil-in-water Pickering emulsions of high oil phase content (WOR = 1) were successfully prepared by combining CNC and a food-grade cationic surfactant, LAE. The binding interactions between CNC and LAE were systematically investigated by ITC along with other techniques. They revealed the profound influence of CNC/LAE complexes on the colloidal behavior of the aqueous suspensions and the stabilization of oil–water interfaces. The surface properties and aggregation state of CNCs, especially in relation to their emulsifying ability, were controllably tuned by incorporating LAE molecules, making the complexes better Pickering stabilizer at proper LAE addition levels. Pickering emulsions were stable against oil coalescence in the presence of small amounts of LAE. At intermediate LAE concentrations, less stable Pickering emulsions were produced, evolving to larger droplet size during storage (droplet creaming to oil coalescence). Further increasing LAE loadings, Pickering emulsions with fine droplets and high stability were obtained. A dual droplet system was observed under such conditions (LAE- and CNC/LAE-stabilized oil droplets). Long-term stability of the prepared Pickering emulsions was attained after storage for at least 1 month. The underlying stabilization mechanism was found to critically depend on the type of complex formed, the type of LAE structure adsorbed on CNC (adsorbed surfactants or admicelles), the presence of free LAE, and the nature of the oil (sunflower and dodecane oils studied in this work). Our results provide an example of an eco-friendly CNC modification strategy by combining a food-grade cationic surfactant and a simple preparing protocol. The successful formulation of edible CNC/LAE-stabilized and concentrated Pickering emulsion paves a way in food manufacturing with tunable and functional properties based on Pickering systems.

ASSOCIATED CONTENT

Supporting Information

The Supporting Information is available free of charge on the ACS Publications website at DOI: 10.1021/acs.biomac.8b00233.

Conductometric titration curve of CNC; morphology of CNC/LAE complexes; rheology and ζ -potential of CNC/LAE-stabilized Pickering emulsions; droplet size distributions of emulsions stabilized by LAE and CNC/LAE complex, respectively; fluorescence images of simultaneous observation of CNC and dodecane in CNC/LAE-stabilized dodecane-in-water emulsion; and visual appearance of CNC/LAE- and LAE-stabilized emulsions after storage, respectively. (PDF)

AUTHOR INFORMATION

Corresponding Authors

*E-mail: orlando.rojas@aalto.fi. Tel: +358-(0)50 512 4227.

*E-mail: long.bai@aalto.fi. Tel: +358-(0)50 339 4495.

ORCID

Long Bai: 0000-0003-3356-9095

Wenchao Xiang: 0000-0003-4281-3109

Siqi Huan: 0000-0003-1688-9484

Orlando J. Rojas: 0000-0003-4036-4020

Author Contributions

The manuscript was written through contributions of all authors. All authors have given approval to the final version of the manuscript.

Notes

The authors declare no competing financial interest.

ACKNOWLEDGMENTS

We acknowledge funding support by the Academy of Finland under the Project SIRAF and TEKES CLIC consortium. This work made use of the facilities of Aalto University's Nanomicroscopy Center. We also acknowledge the Academy of Finland's Center of Excellence HYBER (project 264677) for support to our research programs.

REFERENCES

- (1) McClements, D. J. *Food Emulsions: Principles, Practices, And Techniques*, 2nd ed.; CRC Press: Boca Raton, FL, 2015; p 245.
- (2) Bai, L.; Huan, S.; Gu, J.; McClements, D. J. Fabrication of oil-in-water nanoemulsions by dual-channel microfluidization using natural emulsifiers: Saponins, phospholipids, proteins, and polysaccharides. *Food Hydrocolloids* **2016**, *61*, 703–711.
- (3) Bai, L.; McClements, D. J. Formation and stabilization of nanoemulsions using biosurfactants: Rhamnolipids. *J. Colloid Interface Sci.* **2016**, *479*, 71–79.
- (4) Pickering, S. U. Cxvii-emulsions. *J. Chem. Soc., Trans.* **1907**, *91*, 2001–2021.
- (5) Ramsden, W. Separation of solids in the surface-layers of solutions and 'suspensions' (observations on surface-membranes, bubbles, emulsions, and mechanical coagulation).—preliminary account. *Proc. R. Soc. London* **1903**, *72*, 156–164.
- (6) Aveyard, R.; Binks, B. P.; Clint, J. H. Emulsions stabilised solely by colloidal particles. *Adv. Colloid Interface Sci.* **2003**, *100*, 503–546.
- (7) Peddireddy, K. R.; Nicolai, T.; Benyahia, L.; Capron, I. Stabilization of water-in-water emulsions by nanorods. *ACS Macro Lett.* **2016**, *5*, 283–286.
- (8) Pang, K.; Ding, B.; Liu, X.; Wu, H.; Duan, Y.; Zhang, J. High-yield preparation of a zwitterionically charged chitin nanofiber and its application in a doubly pH-responsive Pickering emulsion. *Green Chem.* **2017**, *19*, 3665–3670.
- (9) Rodier, B.; de Leon, A.; Hemmingsen, C.; Pentzer, E. Controlling Oil-in-Oil Pickering-Type Emulsions Using 2D Materials as Surfactant. *ACS Macro Lett.* **2017**, *6*, 1201–1206.
- (10) Binks, B. P.; Philip, J.; Rodrigues, J. A. Inversion of silica-stabilized emulsions induced by particle concentration. *Langmuir* **2005**, *21*, 3296–3302.
- (11) Ye, F.; Miao, M.; Jiang, B.; Campanella, O. H.; Jin, Z.; Zhang, T. Elucidation of stabilizing oil-in-water Pickering emulsion with different modified maize starch-based nanoparticles. *Food Chem.* **2017**, *229*, 152–158.
- (12) Berton-Carabin, C. C.; Schroën, K. Pickering emulsions for food applications: background, trends, and challenges. *Annu. Rev. Food Sci. Technol.* **2015**, *6*, 263–297.
- (13) Kedzior, S. A.; Dubé, M. A.; Cranston, E. D. Cellulose Nanocrystals and Methyl Cellulose as Co-stabilizers for Nano-

composite Latexes with Double Morphology. *ACS Sustainable Chem. Eng.* **2017**, *5*, 10509–10517.

(14) Habibi, Y.; Lucia, L. A.; Rojas, O. J. Cellulose nanocrystals: chemistry, self-assembly, and applications. *Chem. Rev.* **2010**, *110*, 3479–3500.

(15) Yan, H.; Chen, X.; Song, H.; Li, J.; Feng, Y.; Shi, Z.; Wang, X.; Lin, Q. Synthesis of bacterial cellulose and bacterial cellulose nanocrystals for their applications in the stabilization of olive oil pickering emulsion. *Food Hydrocolloids* **2017**, *72*, 127–135.

(16) Bai, L.; Huan, S.; Xiang, W.; Rojas, O. J. Pickering emulsions by combining cellulose nanofibrils and nanocrystals: Phase behavior and depletion stabilization. *Green Chem.* **2018**, *20*, 1571.

(17) Capron, I.; Rojas, O. J.; Bordes, R. Behavior of nanocelluloses at interfaces. *Curr. Opin. Colloid Interface Sci.* **2017**, *29*, 83–95.

(18) Kalashnikova, I.; Bizot, H.; Cathala, B.; Capron, I. New Pickering emulsions stabilized by bacterial cellulose nanocrystals. *Langmuir* **2011**, *27*, 7471–7479.

(19) Kalashnikova, I.; Bizot, H.; Cathala, B.; Capron, I. Modulation of cellulose nanocrystals amphiphilic properties to stabilize oil/water interface. *Biomacromolecules* **2012**, *13*, 267–275.

(20) Wang, W.; Du, G.; Li, C.; Zhang, H.; Long, Y.; Ni, Y. Preparation of cellulose nanocrystals from asparagus (*Asparagus officinalis* L.) and their applications to palm oil/water Pickering emulsion. *Carbohydr. Polym.* **2016**, *151*, 1–8.

(21) Cherhal, F.; Cousin, F.; Capron, I. Structural description of the interface of Pickering emulsions stabilized by cellulose nanocrystals. *Biomacromolecules* **2016**, *17*, 496–502.

(22) Diamante, L. M.; Lan, T. Absolute viscosities of vegetable oils at different temperatures and shear rate range of 64.5 to 4835 s⁻¹. *J. Food Process* **2014**, *2014*, 1–6.

(23) Zoppe, J. O.; Venditti, R. A.; Rojas, O. J. Pickering emulsions stabilized by cellulose nanocrystals grafted with thermo-responsive polymer brushes. *J. Colloid Interface Sci.* **2012**, *369*, 202–209.

(24) Zhang, Y.; Karimkhani, V.; Makowski, B. T.; Samaranyake, G.; Rowan, S. J. Nanoemulsions and Nanolatexes Stabilized by Hydrophobically Functionalized Cellulose Nanocrystals. *Macromolecules* **2017**, *50*, 6032–6042.

(25) Hu, Z.; Marway, H. S.; Kasem, H.; Pelton, R.; Cranston, E. D. Dried and redispersible cellulose nanocrystal Pickering emulsions. *ACS Macro Lett.* **2016**, *5*, 185–189.

(26) Gómez H., C.; Serpa, A.; Velásquez-Cock, J.; Gañán, P.; Castro, C.; Vélez, L.; Zuluaga, R. Vegetable nanocellulose in food science: A review. *Food Hydrocolloids* **2016**, *57*, 178–186.

(27) Tardy, B. L.; Yokota, S.; Ago, M.; Xiang, W.; Kondo, T.; Bordes, R.; Rojas, O. J. Nanocellulose-Surfactant Interactions. *Curr. Opin. Colloid Interface Sci.* **2017**, *29*, 57–67.

(28) Hu, Z.; Ballinger, S.; Pelton, R.; Cranston, E. D. Surfactant-enhanced cellulose nanocrystal Pickering emulsions. *J. Colloid Interface Sci.* **2015**, *439*, 139–148.

(29) Kedzior, S. A.; Marway, H. S.; Cranston, E. D. Tailoring Cellulose Nanocrystal and Surfactant Behavior in Miniemulsion Polymerization. *Macromolecules* **2017**, *50*, 2645–2655.

(30) Pinazo, A.; Manresa, M.; Marques, A.; Bustelo, M.; Espuny, M.; Perez, L. Amino acid-based surfactants: new antimicrobial agents. *Adv. Colloid Interface Sci.* **2016**, *228*, 17–39.

(31) Ziani, K.; Chang, Y.; McLandsborough, L.; McClements, D. J. Influence of surfactant charge on antimicrobial efficacy of surfactant-stabilized thyme oil nanoemulsions. *J. Agric. Food Chem.* **2011**, *59*, 6247–6255.

(32) Bakal, G.; Diaz, A. The lowdown on lauric arginate. *Food Qual.* **2005**, *12*, 54–61.

(33) Asker, D.; Weiss, J.; McClements, D. Formation and stabilization of antimicrobial delivery systems based on electrostatic complexes of cationic-non-ionic mixed micelles and anionic polysaccharides. *J. Agric. Food Chem.* **2011**, *59*, 1041–1049.

(34) Asker, D.; Weiss, J.; McClements, D. Analysis of the interactions of a cationic surfactant (lauric arginate) with an anionic biopolymer (pectin): isothermal titration calorimetry, light scattering, and microelectrophoresis. *Langmuir* **2009**, *25*, 116–122.

(35) Edgar, C. D.; Gray, D. G. Smooth model cellulose I surfaces from nanocrystal suspensions. *Cellulose* **2003**, *10*, 299–306.

(36) Schneider, C. A.; Rasband, W. S.; Eliceiri, K. W. NIH Image to ImageJ: 25 years of image analysis. *Nat. Methods* **2012**, *9*, 671–675.

(37) Lopez-Pena, C. L.; McClements, D. J. Optimizing delivery systems for cationic biopolymers: Competitive interactions of cationic polylysine with anionic κ -carrageenan and pectin. *Food Chem.* **2014**, *153*, 9–14.

(38) Abitbol, T.; Marway, H.; Cranston, E. D. Surface modification of cellulose nanocrystals with cetyltrimethylammonium bromide. *Nord. Pulp Pap. Res. J.* **2014**, *29*, 46–57.

(39) Huang, L.; Ye, Z.; Berry, R. Modification of Cellulose Nanocrystals with Quaternary Ammonium-Containing Hyperbranched Polyethylene Ionomers by Ionic Assembly. *ACS Sustainable Chem. Eng.* **2016**, *4*, 4937–4950.

(40) Bonnaud, M.; Weiss, J.; McClements, D. J. Interaction of a food-grade cationic surfactant (lauric arginate) with food-grade biopolymers (pectin, carrageenan, xanthan, alginate, dextran, and chitosan). *J. Agric. Food Chem.* **2010**, *58*, 9770–9777.

(41) Arroyo-Maya, I. J.; McClements, D. J. Application of ITC in foods: A powerful tool for understanding the gastrointestinal fate of lipophilic compounds. *Biochim. Biophys. Acta, Gen. Subj.* **2016**, *1860*, 1026–1035.

(42) Brinatti, C.; Huang, J.; Berry, R. M.; Tam, K. C.; Loh, W. Structural and energetic studies on the interaction of cationic surfactants and cellulose nanocrystals. *Langmuir* **2016**, *32*, 689–698.

(43) Dhar, N.; Au, D.; Berry, R. C.; Tam, K. C. Interactions of nanocrystalline cellulose with an oppositely charged surfactant in aqueous medium. *Colloids Surf., A* **2012**, *415*, 310–319.

(44) Chi, K.; Catchmark, J. M. Crystalline nanocellulose/lauric arginate complexes. *Carbohydr. Polym.* **2017**, *175*, 320–329.

(45) Rojas, O. J.; Macakova, L.; Blomberg, E.; Emmer, Å.; Claesson, P. M. Fluorosurfactant self-assembly at solid/liquid interfaces. *Langmuir* **2002**, *18*, 8085–8095.

(46) Penfold, J.; Tucker, I.; Petkov, J.; Thomas, R. Surfactant adsorption onto cellulose surfaces. *Langmuir* **2007**, *23*, 8357–8364.

(47) Wang, C.; Tam, K. New insights on the interaction mechanism within oppositely charged polymer/surfactant systems. *Langmuir* **2002**, *18*, 6484–6490.

(48) Asker, D.; Weiss, J.; McClements, D. Analysis of the interactions of a cationic surfactant (lauric arginate) with an anionic biopolymer (pectin): isothermal titration calorimetry, light scattering, and microelectrophoresis. *Langmuir* **2009**, *25*, 116–122.

(49) Huan, S.; Yokota, S.; Bai, L.; Ago, M.; Borghei, M.; Kondo, T.; Rojas, O. Formulation and composition effects in phase transitions of emulsions co-stabilized by cellulose nanofibrils and an ionic surfactant. *Biomacromolecules* **2017**, *18*, 4393–4404.

(50) Kalashnikova, I.; Bizot, H.; Bertoncini, P.; Cathala, B.; Capron, I. Cellulosic nanorods of various aspect ratios for oil in water Pickering emulsions. *Soft Matter* **2013**, *9*, 952–959.

(51) Bai, L.; Huan, S.; Li, Z.; McClements, D. J. Comparison of emulsifying properties of food-grade polysaccharides in oil-in-water emulsions: Gum arabic, beet pectin, and corn fiber gum. *Food Hydrocolloids* **2017**, *66*, 144–153.